

# Exciton lifetime, Auger recombination, and exciton transport by calibrated differential absorption spectroscopy in $\text{Cu}_2\text{O}$

A. Jolk M. Jörger, and C. Klingshirn

*Institut für Angewandte Physik, Universität Karlsruhe, 76128 Karlsruhe, Germany*

(Received 20 July 2001; published 19 June 2002)

Differential absorption spectroscopy shows a characteristic dependence on the density of 1s excitons in  $\text{Cu}_2\text{O}$  at low temperature. The relation between absorption change and 1s exciton density is established and calibrated using one- and two-photon excitation. The calibrated density evaluation is applied to exciton transport measurements in a quasi-one-dimensional sample geometry. A numerical simulation of the transport yields extremely long exciton lifetimes of up to 3 ns. The Auger recombination of excitons is almost negligible, contrary to previous estimates. A deviation of the transport characteristics from the diffusive regime was not observed.

DOI: 10.1103/PhysRevB.65.245209

PACS number(s): 78.47.+p, 72.90.+y

## I. INTRODUCTION

For several years,  $\text{Cu}_2\text{O}$  has been at the center of the research of Bose-Einstein condensation (BEC) of excitons. Although several distinct experiments have claimed evidence for BEC, discussion has always continued whether indeed the observed phenomena could be unambiguously attributed to nonclassical statistics.<sup>1-6</sup> Recently, even older results have been doubted because a well-known exciton loss mechanism, namely, the Auger recombination, was found to be two orders of magnitude stronger than previously assumed.<sup>7,8</sup> At very high densities of excitons (around  $10^{17} \text{ cm}^{-3}$ ), this process tends to limit the exciton density to values well below the critical BEC threshold.

The most promising experimental technique for condensation studies is the analysis of exciton transport. At exciton densities above the condensation threshold, a change in the propagation characteristics from diffusive transport to a ballistic regime has been reported.<sup>1</sup> While the interpretation of a ballistic transport as a sign of superfluidity and thus BEC has been doubted, it is certainly an incentive for further research into the transport properties of a dense nonhomogeneous exciton cloud.

In the present paper, we measure the density of excitons as a function of space and time using a previously developed all-optical detection method. This method relies on the fact that a high density of 1s excitons leads to a change in the absorption spectrum of  $\text{Cu}_2\text{O}$  in the spectral range of the  $np$  exciton states.<sup>9</sup> The relevant processes are exciton-exciton scattering and Coulomb screening by a polarizable exciton gas. While no detailed theory of these processes has been developed, it is assumed that the two species of 1s excitons, namely, orthoexcitons and paraexcitons, are indistinguishable in this setup and contribute equally to the absorption change. This statement is correct for Coulomb screening. There might be some spin dependence in Pauli blocking; but since excitons in  $\text{Cu}_2\text{O}$  are small ( $a_B \approx 0.7 \text{ nm}$ ) and because we deal with a three-dimensional case, the second contribution to screening is much smaller than the first one (see e.g. Ref. 10 and references therein).

The exact functional relation between the change in ab-

sorption and the corresponding density of 1s excitons has been established in a series of pump-probe type experiments. In these experiments, the absorption spectrum is measured during or shortly after excitation with an intense laser pulse, on a time scale where the created exciton density is not influenced by diffusion or recombination. Exciton densities of up to  $10^{19} \text{ cm}^{-3}$  were reached by one-photon excitation above the band gap, thus creating free carriers that efficiently recombine to excitons. Even higher densities up to  $10^{20} \text{ cm}^{-3}$  were obtained using two-photon absorption of a terawatt infrared laser pulse at half the 1s exciton resonance energy, thus creating a cold exciton population near  $\vec{k}=0$ .

The propagation of excitons through a quasi-one-dimensional sample was studied and modeled in the diffusive approximation. While no indications for nondiffusive transport were found, we were able to fit values for exciton lifetime and the Auger recombination coefficient which show that Auger recombination is several orders of magnitude lower than previously assumed.

It is important to bear in mind that the absolute value of the Auger coefficient depends linearly on the initial exciton density estimation. As a consequence, special attention has to be paid to the reliability of the exciton density evaluation.

## II. EXPERIMENTAL SETUP

### A. One-photon excitation

For pump-probe-type experiments with one-photon excitation, excitons were created using a nitrogen-laser pumped dye laser at 560 nm with a pulse duration of 5 ns. The maximum excitation intensity was  $20 \text{ MW/cm}^2$ . Assuming an exciton formation efficiency of one exciton per absorbed photon and a penetration depth of  $35 \mu\text{m}$ , the maximum exciton density is  $n_X = 8 \times 10^{19} \text{ cm}^{-3}$ . During the short duration of the exciting laser pulse, spontaneous recombination of single excitons cannot significantly reduce the total number of particles. The postulated high values of the Auger recombination coefficient would lead to an effective exciton lifetime that is much shorter than the laser pulse; this possibility can be ruled out by the results from the two-photon excitation experiments that used a pulse duration of only 100 fs. Fur-

thermore, it would be completely impossible to explain the existence of sufficient exciton densities to produce significant bleaching even after 1 ms as shown later.

As for surface recombination, assuming an exciton diffusion velocity below  $10^5$  cm/s, only those excitons created in a volume extending  $5 \mu\text{m}$  below the sample surface can reach the surface during the laser pulse. Even if surface recombination were arbitrarily fast, the maximum error in initial exciton density does not exceed 20%.

The probe beam was the spontaneous emission of a dye cuvette that was quenched to about 3 ns length and optically delayed to arrive during the pump pulse. The sample was a polished  $\text{Cu}_2\text{O}$  platelet of  $50 \mu\text{m}$  thickness on a sapphire support. It was cooled in a liquid helium (LHe) exchange gas cryostat. The platelet was cut from the same naturally grown  $\text{Cu}_2\text{O}$  single crystal as all subsequent samples. This sample was selected by the linear absorption spectrum, showing the  $np$  exciton series up to the  $n=9$  state. Even though the sample was glued to a sapphire support, no strain-induced effects such as line shift or increased 1s absorption were observed.

### B. Two-photon excitation

Experiments using a two-photon excited exciton population were performed in the ENSTA in Palaiseau (France). A three-stage optical parametrical amplifier (OPA) was pumped by 30 fs,  $100 \mu\text{J}$ , 800 nm pulses from the second stage of a chirped-pulse amplification laser system. The OPA was tuned to a central wavelength of 1270 nm and delivered pulses of  $40 \mu\text{J}$  pulse energy and a duration of 100 fs at a repetition rate of 10 Hz. These pulses were split into two counterpropagating beams and circularly polarized. Optical delay lines were used to guarantee simultaneous incidence of both pulses on the sample surface.

Part of the 800 nm stray light from the OPA was focused inside a 3 mm Suprasil glass in order to create a short white light continuum. It was transmitted through the excited sample volume under a small angle and collected onto the entrance slit of a grating spectrometer.

The sample was a chemically polished free platelet with  $50 \mu\text{m}$  thickness held at either  $T=2$  K or 6 K in LHe exchange gas.

Assuming an exciton formation efficiency of one exciton per two absorbed photons, the exciton density can be calculated from the differential equation for two-photon absorption

$$\frac{dI}{dx} = -\alpha I - \beta I^2. \quad (1)$$

Neglecting the one-photon absorption  $\alpha$  in the infrared spectral range, the solution of Eq. (1) is

$$I(x) = \frac{I_0}{1 + \beta I_0 x}, \quad (2)$$

where  $I_0$  is the incident intensity. At a laser-pulse energy of  $20 \mu\text{J}$  in 100 fs and a spot diameter of 0.1 mm,  $I_0 = 2.5 \times 10^{12}$  W/cm<sup>2</sup>. The average density of the 1s excitons

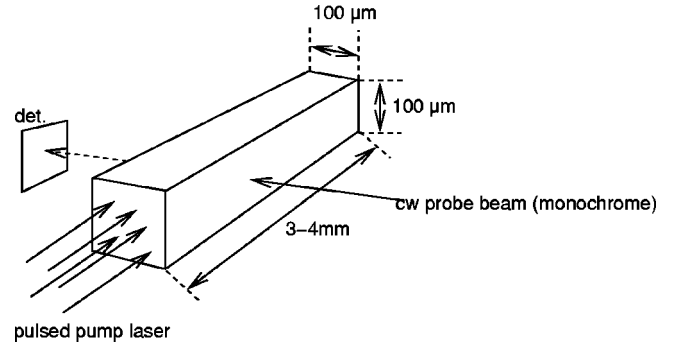


FIG. 1. Experimental setup for the transport measurements.

created in the sample volume between depths  $x_1$  and  $x_2$  measured from the surface, thus neglecting the regions near the surface where loss mechanisms might intervene, results from an integration of Eq. (2) to

$$n_x = \frac{\tau_{\text{pulse}} \beta I_0^2}{\hbar \omega_1 (1 + \beta I_0 x_1) (1 + \beta I_0 x_2)}, \quad (3)$$

where  $\hbar \omega_1 = 2.033\text{eV}$  is the energy of the resonantly created excitons and  $\tau_{\text{pulse}}$  is the pump-laser duration. For our density evaluations, we used values of  $x_1 = 1 \mu\text{m}$  and  $x_2 = 49 \mu\text{m}$ , thus neglecting the influence of the volume within  $1 \mu\text{m}$  from the sample surface. The two-photon absorption coefficient has been estimated from the infrared pump-laser transmission to  $\beta = 0.001$  cm/MW.

In order to rule out any possible oversight of Auger recombination, the differential absorption spectrum was recorded with a time-delayed probe pulse up to 15 ps after the exciton creation. During this time, no significant decay of the induced absorption was detectable. Assuming a worst-case error of one order of magnitude, this observation alone gives an upper limit for the Auger coefficient of  $A = 10^{-17}$  cm<sup>3</sup>/ns.

### C. Transport measurements

For the transport measurements, a long crystal rod was prepared with a square cross section of  $100 \mu\text{m}$  side length and a length of about 3 mm. The rod was glued to a sapphire support. The pump laser was focused onto the polished abutting face. The probe beam was a weak continuous-wave (cw) dye laser beam transmitted perpendicularly through the sample at a variable distance from the excited surface. Figure 1 gives a schematic of the experimental idea. The sample was held at various temperatures between 2 K and 30 K in a LHe exchange gas cryostat.

The pump laser was an excimer laser pumped dye laser with 10 ns pulse duration at a wavelength of 555 nm. Typical excitation intensities reached  $30 \text{ MW/cm}^2$ .

The probe laser was an argon-ion laser pumped tunable cw dye laser. It was tuned to several wavelengths in the spectral range of the  $np$  excitons and was filtered to an intensity well below the mean pump-laser intensity.

It has to be noted that in this particular sample geometry, the effect of an increased surface recombination cannot be distinguished from a merely intrinsic recombination, because

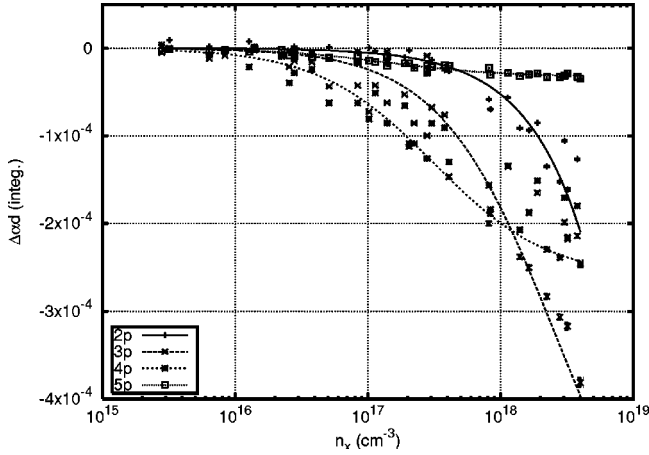


FIG. 2. Fit of Eq. (4) to the 2p-5p exciton lines, for one-photon experiments with an effective pumped thickness of 35  $\mu\text{m}$ . The 5p line is in saturation for almost all densities; its lower value is due to the lower oscillation strength of the 5p exciton line.

the exciton detection integrates over the complete cross section of the crystal rod. Since we find a total exciton lifetime of up to several milliseconds, we can safely neglect this eventual contribution.

### III. EXCITON DENSITY CALIBRATION

The differential absorption was spectrally integrated over various  $np$  exciton lines and plotted against 1s exciton density. The resulting curves as shown in Fig. 2 for a 35  $\mu\text{m}$  sample fit very well to a phenomenological description of the form

$$(\Delta\alpha d)_{\text{int}}(n_X) = \frac{a_c}{1 + n_c/n_X}, \quad (4)$$

where  $n_X$  is the 1s exciton density,  $n_c$  is a critical density for the respective  $np$  exciton resonance, and  $a_c$  is a saturation parameter. One- and two-photon excitation experiments give good agreement for the critical densities, within an error in-

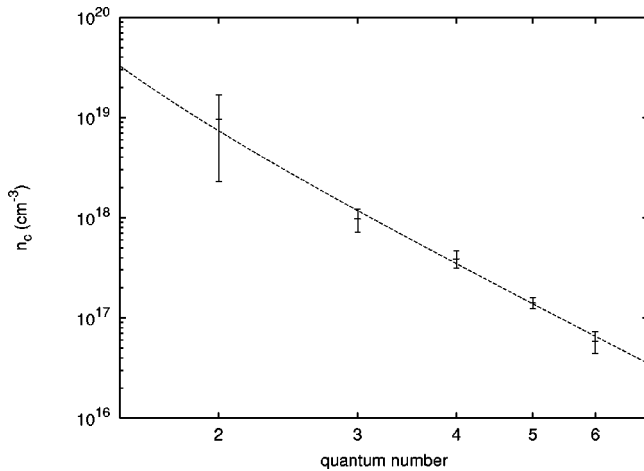


FIG. 3. Fit of the critical density  $n_c^{(n)}$  for  $n=2, \dots, 6$  to a Mott criterion.

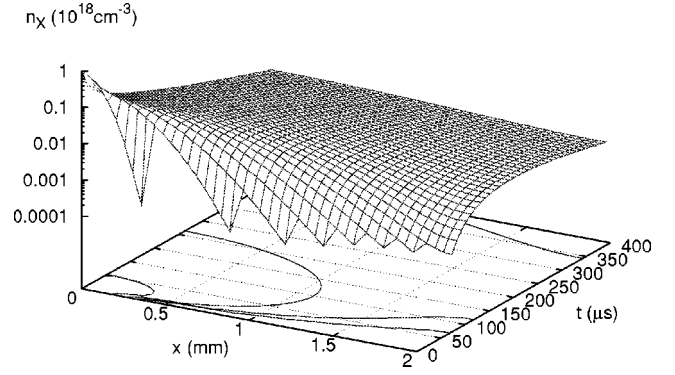


FIG. 4. Solution of the diffusion equation with finite exciton lifetime and Auger recombination. At  $t=0$ ,  $n_X(0,0) = 10^{19} \text{ cm}^{-3}$  at the excited surface and  $n_X=0$  in the volume. Simulation parameters: exciton lifetime  $\tau_X = 100 \mu\text{s}$ , Auger coefficient  $A = 2 \times 10^{-23} \text{ cm}^3/\text{ns}$ , diffusion coefficient  $D = 20 \text{ cm}^2/\text{s}$ .

terval not exceeding a factor of 2. The one- and two-photon excitation experiments are independent. Especially the second kind produces volume excitation with only marginal influence of surface recombination, and negligible Auger recombination even if one assumes the highest postulated values of the Auger coefficient. Therefore the absolute values of the exciton density are correct within half an order of magnitude.

The critical or Mott density  $n_c^{(n)}$  for the different  $np$  lines is expected to be related to the radius  $a_n$  of the  $np$  excitons following

$$n_c^{(n)} = a_n^{-3} = \left[ a_B \left( \frac{3}{2} n^2 - 1 \right) \right]^{-3}. \quad (5)$$

Here,  $a_B$  is the Bohr radius of the  $np$  excitons, and the relation between  $a_n$  and  $a_B$  holds for hydrogenlike p states.

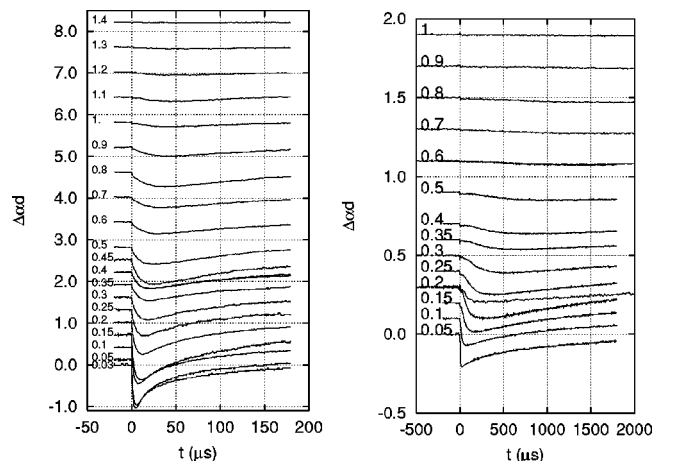


FIG. 5. Differential absorption as a function of time for  $T=2 \text{ K}$  (left) and  $T=30 \text{ K}$  (right). The curves for different distance from the excited surface as given in the plot (in mm) are set off vertically for clarity. The minimum of differential absorption shifts to later times with increasing distance and broadens considerably. At  $T=2 \text{ K}$ , the propagation is noticeably faster (note the different scales on the abscissa).

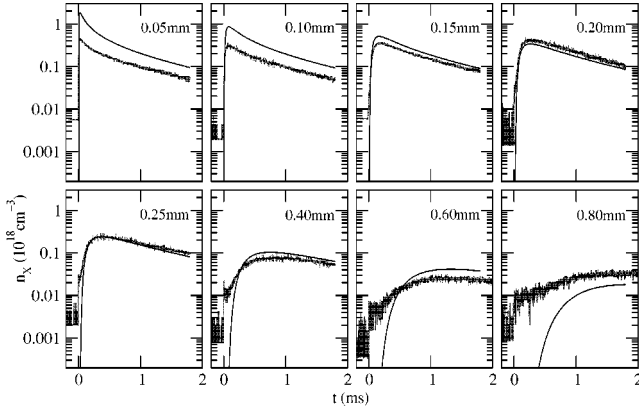


FIG. 6. Comparison of experimental data and numerical simulation at  $T=30$  K. Simulation parameters were  $D=0.5$  cm<sup>2</sup>/s,  $A=10^{-24}$  cm<sup>3</sup>/ns, and  $\tau=2$  ms. The respective distance  $x$  of the detection (probe) spot to the excited surface is given in the plots.

A fit of this equation (Fig. 3) yields  $a_B=1.7(2)$  nm and  $n_c \propto a_n^{-2}$ . The value of  $a_B$  agrees reasonably with the accepted value of 1.1 nm for p-type excitons. This fit represents another independent verification of our exciton density estimate within a factor of 4.

#### IV. TRANSPORT EXPERIMENTS

##### A. Numerical simulation of diffusion

The diffusive propagation of excitons can be described with a diffusion equation of the form

$$\frac{\partial n_X}{\partial t} = -D \frac{\partial^2 n_X}{\partial x^2}, \quad (6)$$

where  $D$  is the diffusion coefficient. This equation assumes that the mean free path of the excitons is short in comparison with the volume of the crystal, and that the diffusion coefficient  $D$  is independent from the density. In a superfluid condensate, these approximations are expected to break down.

Additionally, a finite exciton lifetime leads to losses following  $k_\tau n_X$  (where  $k_\tau^{-1} = \tau_X$  is the exciton lifetime); Auger

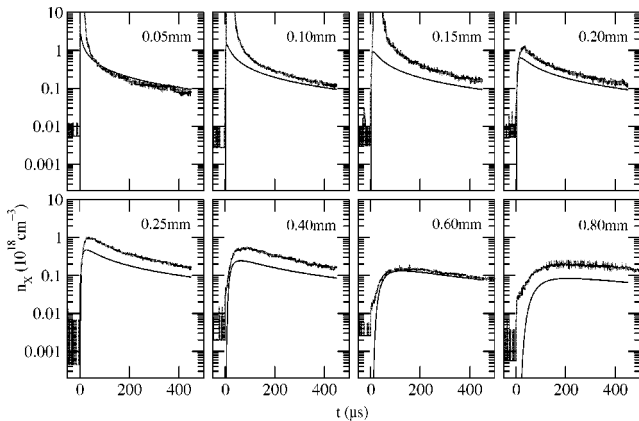


FIG. 7. Same comparison as in Fig. 6 for  $T=15$  K. Simulation parameters:  $D=8$  cm<sup>2</sup>/s,  $A=10^{-23}$  cm<sup>3</sup>/ns, and  $\tau=3$  ms.

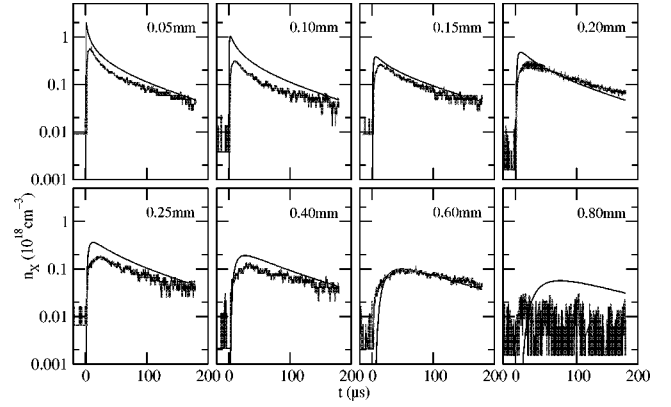


FIG. 8. Same comparison as in Fig. 6 for  $T=6$  K. Simulation parameters  $D=20$  cm<sup>2</sup>/s,  $A=10^{-23}$  cm<sup>3</sup>/ns, and  $\tau=150$  μs.

losses lead to a term  $An_X^2$ . Additional surface recombination has been neglected for the reasons cited above. The resulting complete differential equation reads

$$\frac{\partial n_X}{\partial t} = -D \frac{\partial^2 n_X}{\partial x^2} - k_\tau n_X - An_X^2. \quad (7)$$

The solution of Eq. 7 is plotted in Fig. 4 for typical parameters.

##### B. Experimental results

Figure 5 gives the differential absorption as a function of time at different distances from the excited surface, at  $T=2$  K (left) and  $T=30$  K (right). The probe laser was tuned to  $\hbar\omega=2.1677$  eV in the 4p resonance. Exciton transport over distances up to 0.8 mm at 30 K and 1.2 mm at 2 K is clearly visible. The propagation is faster by about an order of magnitude at  $T=2$  K.

By comparing the experimental results with the simulation of diffusive transport, the exciton lifetime as well as the diffusion and Auger coefficients can be determined. The calibration function [inverse of Eq. (4)] is applied to the measured differential absorption for different distances  $x$ , yielding the time-resolved exciton density  $n_X(t)$ . The initial exciton density  $n_X(x=0, t=0)$  is calculated from the ab-

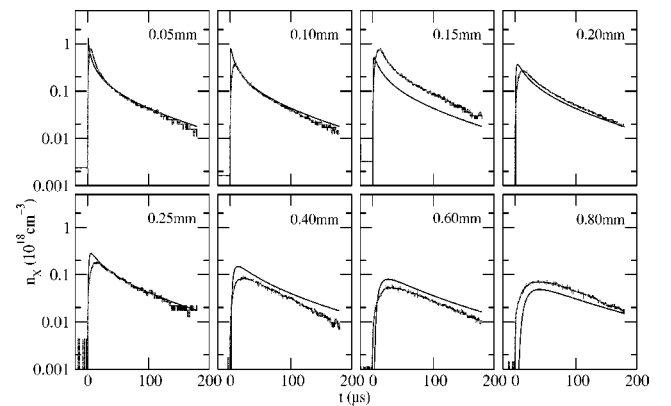


FIG. 9. Same comparison as in Fig. 6 for  $T=2$  K. Simulation parameters  $D=40$  cm<sup>2</sup>/s,  $A=5 \times 10^{-23}$  cm<sup>3</sup>/ns, and  $\tau=150$  μs.

sorbed pump energy as justified by the investigations in Sec. III above. A first guess of the excitonic lifetime  $\tau$  can be obtained as an exponential fit to the density decrease at large times  $t$ . The diffusion coefficient  $D$  influences prominently the arrival time of the maximum for large distances  $x$ , and the Auger coefficient  $A$  has a pronounced effect only on the high densities observed at small distance  $x$  and small times  $t$ .

Figures 6–9 compare the fitted simulations to experimental data for four different temperatures. Simulation parameters have been chosen so as to fit the set of all distances equally well. It is observed that the diffusion constant increases as expected with decreasing temperature, whereas the Auger recombination has only little influence for all temperatures. The exciton lifetime decreases by an order of magnitude at low temperature compared to  $T = 30$  K.

## V. DISCUSSION

The agreement between experimental data and calculated diffusion in Figs. 6–9 is equally good for all temperatures. The reported diffusion coefficient is lower by about an order of magnitude than the accepted value.<sup>11</sup> The temperature dependence nearly agrees with the reported  $T^{-3/2}$  behavior. An effective exciton temperature higher than the lattice temperature cannot explain this difference because excitons are known to thermalize on a nanosecond time scale with the lattice. Moreover, the relative difference between the lattice and exciton temperatures should diminish with increasing temperature. Possible reasons for the discrepancy of the absolute values might be nonspecular scattering of excitons at the sample surfaces or strain-induced TA-phonon scattering.<sup>11</sup>

The value of the Auger coefficient  $A$  is smaller by several orders of magnitude than both the previously accepted value of  $A = 10^{-18}$  cm<sup>3</sup>/ns (Refs. 12,13) and the value reported by Wolfe *et al.*<sup>7,8</sup> of  $A = 10^{-16}$  cm<sup>3</sup>/ns. Recent calculations<sup>14</sup> show that the Auger recombination rate should indeed become negligible given a long paraexciton lifetime. The dominant loss process for orthoexcitons is thus not exciton annihilation by energy transfer to another exciton, but rather conversion of two orthoexcitons into two paraexcitons by particle exchange. This process conserves the total number of excitons but decreases the orthoexciton number and thus the photoluminescence intensity. It is favored by the fact that the ortho-para splitting is close to an LO-phonon energy and that a biexciton state with vanishing binding energy<sup>15</sup> may act as a virtual, resonant intermediate level.

A high value of  $A$  would lead to an almost instantaneous density drop, given the observed densities; assuming  $A = 10^{17}$  cm<sup>3</sup>/ns, at a density of  $n_X = 10^{17}$  cm<sup>-3</sup> the initial effective lifetime would be 1 ns only, contrary to our observations. As noted before, the fit value of  $A$  scales with the absolute exciton density. Thus, the maximal uncertainty of the absolute exciton density of a factor of 4 limits the error of  $A$  to the same factor of 4, incommensurable with the deviation of several orders of magnitude with respect to earlier estimates. The correct order of magnitude of the exciton density was verified by the Mott fit (Fig. 3).

The density calibration assumed an exciton formation ef-

iciency of 1 which was previously reported by several groups.<sup>16,17</sup> The known exciton dynamics does not propose any other efficient recombination channel for free carriers besides exciton formation and relaxation.<sup>18</sup>

Our measurements give clear evidence that Auger recombination is a negligible exciton loss mechanism even at densities in the  $10^{18}$  cm<sup>-3</sup> range. The orthoexciton loss observed in luminescence is explained by conversion into the paraexciton state. It seems reasonable that a small and electrically neutral particle like the 1s exciton, not even having a dipole moment, shows a very small Auger scattering rate. This result is in accordance with recent work by Denev and Snoke.<sup>19</sup>

A further ortho-para relaxation mechanism is phonon emission.<sup>20,21</sup> Since phonons do not primarily interact with the spin this process is relatively slow. Therefore it may dominate at low densities, while the spin-exchange process depends on the square of the exciton density and should therefore dominate at high densities.

The observed exciton lifetime shows qualitatively good agreement with the temperature dependence and the minimum in luminescence quantum efficiency.<sup>20,22</sup> The lifetime change follows the temperature dependence of the orthoexciton-paraexciton conversion. At low temperature, the conversion from ortho- to paraexciton is frozen; the generated excitons predominantly remain in the orthoexciton state and decay with the orthoexciton lifetime. At higher temperature around 15 K, orthoexciton to paraexciton down-conversion is efficient, and the observed lifetime is the paraexciton lifetime. At still higher temperatures of 30 K and more, thermal paraexciton to orthoexciton up-conversion opens an additional recombination channel for the paraexcitons, which leads to a slightly reduced lifetime.

From our data, no deviation from classical transport can be inferred, even though at  $T = 2$  K the exciton density exceeds the critical density for BEC of an ideal gas, which is  $n_X = 10^{17}$  cm<sup>-3</sup> for paraexcitons. Other groups have reported a characteristic change in transport properties for comparable excitation conditions.<sup>1–3,23–25</sup> The low value of the diffusion coefficient raises the suspicion that the sample was slightly strained, which might inhibit the formation of a condensate.

The lack of the observation of nonclassical propagation in our experiments could also be explained by a certain fraction of excitons in a fast-moving condensate which crosses the detection spot within a few hundreds of nanoseconds, too fast for our detection system to resolve. The simulations in Figs. 6–9, however, seem to account for all created excitons. If the eventual condensate comprises only part of the created excitons, uncertainties in the absolute density calibration could overestimate the density in the remaining diffusive cloud, covering the fact that a large fraction of the created excitons are missing. Current estimates of the condensate fraction are of a few percent.<sup>26,27</sup>

Another possibility is that excitons in a Bose condensed state might no longer contribute to screening. It is, however, not obvious from first principles whether a condensate should be more or less efficient in screening compared to a classical gas.<sup>28</sup>

## VI. CONCLUSIONS

Our measurements give no indication of a nonclassical superfluid transport, even under excitation conditions where other groups reported ballistic transport. It is possible that fast ballistic transport of only part of the created excitons remains invisible in our experiments, with the noncondensate fraction showing classical diffusive transport. An increase of the pump power and an improved detection system could reveal the existence of this ballistic part. A comparison of the optical measurements as shown here and the electrical ones of Refs. 1–3 on one and the same sample are planned and will give decisive evidence of the nature of the transport.<sup>18</sup>

The Auger coefficient has been demonstrated to be considerably smaller than previously reported. In particular, we find exciton lifetimes of  $\tau=150 \mu\text{s}$  at  $T=2 \text{ K}$  and at densities around  $10^{17} \text{ cm}^{-3}$ ; at  $T=15 \text{ K}$ , the exciton lifetime reaches  $\tau=3 \text{ ms}$ .

## ACKNOWLEDGMENTS

We thank Dr. G. Kavoulakis for very fruitful discussions and Prof. Dr. A. Mysyrowicz for critical and stimulating discussions and for allowing us to access the laser infrastructure in Palaiseau. A.J. acknowledges financial support by the Deutsche Forschungsgemeinschaft.

- 
- <sup>1</sup>E. Benson, E. Fortin, and A. Mysyrowicz, *Phys. Status Solidi B* **191**, 345 (1995).  
<sup>2</sup>E. Benson, E. Fortin, and A. Mysyrowicz, *Solid State Commun.* **101**, 313 (1997).  
<sup>3</sup>E. Benson, E. Fortin, B. Prade, and A. Mysyrowicz, *Europhys. Lett.* **40**, 311 (1997).  
<sup>4</sup>G.A. Kopelevich, S.G. Tikhodeev, and N.A. Gippius, *JETP* **82**, 1180 (1996).  
<sup>5</sup>G.A. Kopelevich, N.A. Gippius, and S.G. Tikhodeev, *Solid State Commun.* **99**, 93 (1996).  
<sup>6</sup>S.G. Tikhodeev, G.A. Kopelevich, and N.A. Gippius, *Phys. Status Solidi B* **206**, 45 (1998).  
<sup>7</sup>K.E. O'Hara and J.P. Wolfe, *Phys. Rev. B* **62**, 12 909 (2000).  
<sup>8</sup>J.T. Warren, K.E. O'Hara, and J.P. Wolfe, *Phys. Rev. B* **61**, 8215 (2000).  
<sup>9</sup>A. Jolk and C.F. Klingshirn, *Phys. Status Solidi B* **206**, 841 (1998).  
<sup>10</sup>C. F. Klingshirn, *Semiconductor Optics* (Springer-Verlag, Heidelberg, 1995).  
<sup>11</sup>D.P. Trauernicht, J.P. Wolfe, and A. Mysyrowicz, *Phys. Rev. Lett.* **52**, 855 (1984).  
<sup>12</sup>G.M. Kavoulakis and G. Baym, *Phys. Rev. B* **54**, 16 625 (1996).  
<sup>13</sup>G.M. Kavoulakis, G. Baym, and J.P. Wolfe, *Phys. Rev. B* **53**, 7227 (1996).  
<sup>14</sup>G. Kavoulakis and A. Mysyrowicz, *Phys. Rev. B* **61**, 16 619 (2000).  
<sup>15</sup>F. Bassani and M. Rovere, *Solid State Commun.* **19**, 887 (1976).  
<sup>16</sup>E. Fortin, S. Fafard, and A. Mysyrowicz, *Phys. Rev. Lett.* **70**, 3951 (1993).  
<sup>17</sup>K.E. O'Hara, J.R. Gullingsrud, and J.P. Wolfe, *Phys. Rev. B* **60**, 10 872 (1999).  
<sup>18</sup>J. P. Wolfe, J. L. Lin, and D. W. Snoke, in *Bose-Einstein Condensation*, 1st ed., edited by A. Griffin, D. W. Snoke, and S. Stringari (Cambridge University Press, Cambridge, England, 1995), Chap. 13, pp. 281–329.  
<sup>19</sup>S. Denev and D.W. Snoke, *Phys. Rev. B* **65**, 085211 (2002).  
<sup>20</sup>N. Caswell and P.Y. Yu, *Phys. Rev. B* **25**, 5519 (1982).  
<sup>21</sup>D.W. Snoke, D.P. Trauernicht, and J.P. Wolfe, *Phys. Rev. B* **41**, 5266 (1990).  
<sup>22</sup>M. Jörger, M. Schmidt, A. Jolk, R. Westphäling, and C. Klingshirn, *Phys. Rev. B* **64**, 113204 (2001).  
<sup>23</sup>E. Fortin, E. Benson, and A. Mysyrowicz, in *Bose-Einstein Condensation* (Ref. 18), Chap. 27, pp. 519–523.  
<sup>24</sup>E. Fortin and A. Mysyrowicz, in *1999 International Conference on Luminescence and Optical Spectroscopy of Condensed Matter*, edited by K. Cho [*J. Lumin.* **87-89**, 12 (2000)].  
<sup>25</sup>A. Mysyrowicz, E. Fortin, E. Benson, and S. Fafard, *Solid State Commun.* **92**, 957 (1994).  
<sup>26</sup>E. Benson, Ph.D. thesis, University of Ottawa, 1999.  
<sup>27</sup>H. Haug and H.H. Kranz, *Z. Phys. B: Condens. Matter* **53**, 151 (1983).  
<sup>28</sup>H. Haug, R. Zimmermann, G. Kavoulakis, and P. Littlewood (private communications).